

## Research



**Cite this article:** Heydarizadeh P *et al.* 2017  
Response of CO<sub>2</sub>-starved diatom *Phaeodactylum*  
*tricornutum* to light intensity transition. *Phil.*  
*Trans. R. Soc. B* **372**: 20160396.  
<http://dx.doi.org/10.1098/rstb.2016.0396>

Accepted: 1 June 2017

One contribution of 16 to a theme issue 'The  
peculiar carbon metabolism in diatoms'.

**Subject Areas:**

molecular biology, plant science,  
environmental science, cellular biology

**Keywords:**

*Phaeodactylum tricornutum*,  
carbon metabolism, light regulation,  
photosynthesis, chlorophyll fluorescence,  
pyruvate hub

**Author for correspondence:**

Benoît Schoefs  
e-mail: [benoit.schoefs@univ-lemans.fr](mailto:benoit.schoefs@univ-lemans.fr)

Electronic supplementary material is available  
online at [https://dx.doi.org/10.6084/m9.  
figshare.c.3800485](https://dx.doi.org/10.6084/m9.figshare.c.3800485).

# Response of CO<sub>2</sub>-starved diatom *Phaeodactylum tricornutum* to light intensity transition

Parisa Heydarizadeh<sup>1</sup>, Wafâa Boureba<sup>1</sup>, Morteza Zahedi<sup>2</sup>, Bing Huang<sup>1</sup>,  
Brigitte Moreau<sup>1</sup>, Ewa Lukomska<sup>3</sup>, Aurélie Couzinet-Mossion<sup>4</sup>,  
Gaëtane Wielgosz-Collin<sup>4</sup>, Véronique Martin-Jézéquel<sup>5</sup>, Gaël Bougaran<sup>3</sup>,  
Justine Marchand<sup>1</sup> and Benoît Schoefs<sup>1</sup>

<sup>1</sup>Metabolism, Bioengineering of Microalga Molecules and Applications (MIMMA), Mer Molécules Santé, UBL, IUML-FR 3473 CNRS, University of Le Mans, 72085 Le Mans, France

<sup>2</sup>Department of Agronomy and Plant Breeding, College of Agriculture, Isfahan University of Technology, Isfahan 84156-83111, Iran

<sup>3</sup>FREMER, Physiology and Biotechnology of Algae Laboratory, rue de l'Île d'Yeu, BP 21105, 44311 Nantes, France

<sup>4</sup>Faculté des Sciences Pharmaceutiques et Biologiques, Université de Nantes, Groupe Mer, Molécules, Santé-EA 2160, Institut Universitaire Mer et Littoral FR3473 CNRS, 9 rue Bias, BP 61112, 44035 Nantes Cedex 1, France

<sup>5</sup>UMR 7266-CNRS LIENSs, Université de La Rochelle, 2 rue Olympe de Gouges, 17000 La Rochelle, France

PH, 0000-0002-6510-7103; BS, 0000-0002-7804-8130

In this study, we investigated the responses of *Phaeodactylum tricornutum* cells acclimated to 300  $\mu\text{mol m}^{-2} \text{s}^{-1}$  photon flux density to an increase (1000  $\mu\text{mol m}^{-2} \text{s}^{-1}$ ) or decrease (30  $\mu\text{mol m}^{-2} \text{s}^{-1}$ ) in photon flux densities. The light shift occurred abruptly after 5 days of growth and the acclimation to new conditions was followed during the next 6 days at the physiological and molecular levels. The molecular data reflect a rearrangement of carbon metabolism towards the production of phosphoenolpyruvic acid (PEP) and/or pyruvate. These intermediates were used differently by the cell as a function of the photon flux density: under low light, photosynthesis was depressed while respiration was increased. Under high light, lipids and proteins accumulated. Of great interest, under high light, the genes coding for the synthesis of aromatic amino acids and phenolic compounds were upregulated suggesting that the shikimate pathway was activated.

This article is part of the themed issue 'The peculiar carbon metabolism in diatoms'.

## 1. Background

Light is a driving force behind biomass production by photosynthetic organisms. Variation of the light regime strongly affects microalga ecology, physiology, chemical composition and gene expression. Therefore, manipulation of light appears to be an attractive tool for enhancing growth of microalgae in order to extend the use of these organisms in biotechnology [1–3]. Diatoms constitute one of the most abundant and diversified groups of microalgae. Diatoms are particularly adapted to grow in very dynamic environments, suggesting they have sophisticated mechanisms to perceive and rapidly respond to environmental variations [4–6]. Understanding molecular and physiological responses of diatoms to fluctuations in light fluxes is important for parametrizing models of photosynthetic productivity, providing directions for improvements of overall biomass yields and for engineering superior strains or cultivation methods [7]. The availability of the genome [8], transcriptomic and proteomic data of *Phaeodactylum tricornutum* exposed to different stimuli including light [9–11], oxidative [12] and nutrient stresses [13–15] made this species a model of choice to study the existence of adaptive strategies in diatoms. For instance,

*P. tricornutum* has the capacity to survive in darkness for a long period [16], maintaining a functional photosynthetic apparatus during dark periods, and promptly recovers upon re-illumination [10]. *Phaeodactylum* responds to changes in light exposure through physiological upregulation and down-regulation mechanisms. Long-term mechanisms (hours to days), generally designated as photoacclimation, include changes in the levels of photosynthetic pigments, electron transport chain components, enzymes of carbon metabolism and/or non-photochemical quenching [9,17–22]. Non-photochemical quenching designates a set of photoprotective mechanisms that relies on the generation of  $\Delta\text{pH}$  between the thylakoid lumen and the chloroplast stroma during light exposure, and back conversion in its absence (i.e. typically in the dark). Nuclear-encoded LhcX proteins are involved in the non-photochemical quenching in the pennate diatom *P. tricornutum* [18,19] and the centric diatom *Thalassiosira pseudonana* [20,21]. Each of these mechanisms develops under a certain time frame. Roháček *et al.* [22] have established a mathematical method that allows the determination of the intensity of fast, intermediate and slow non-photochemical components. Still, molecular mechanisms behind photoacclimation in diatoms are largely unknown, especially those involved in photoacclimation to low photon flux densities. For instance, Nymark *et al.* [17] studied the photoacclimation of *P. tricornutum* during the first 48 h following an increase of low to medium photon flux density. In this time frame, the major differences concerned the photosynthetic machinery involved in the photochemical phase of photosynthesis while the biochemical phase of photosynthesis, i.e. the Calvin cycle, remained mostly unaffected [17]. On the other hand, under stress conditions, diatoms may reorient their metabolism towards the production of lipids [23]. This process is enhanced in the presence of high  $\text{CO}_2$  concentration [24]. While it has been shown that light exerts a control on this phenomenon [25], it has not been investigated whether the  $\text{CO}_2$  availability also plays a regulatory role. To address this question, we conducted an integrated analysis combining pigment, lipid and protein quantification, activity and efficiency of photosynthesis, photoprotection mechanisms and transcription levels of genes important for carbon metabolism, in axenically grown *P. tricornutum* under  $\text{CO}_2$ -limited conditions when  $300 \mu\text{mol photon m}^{-2} \text{s}^{-1}$  (medium light, ML) acclimated cells are shifted to  $30 \mu\text{mol photon m}^{-2} \text{s}^{-1}$  (low light, LL) or  $1000 \mu\text{mol photon m}^{-2} \text{s}^{-1}$  (high light, HL) for a period of 6 days. This information contributes to the understanding of the carbon partitioning in diatom cells and opens doors to improvement of microalgal biotechnological processes for production of biomolecules [26].

## 2. Material and methods

### (a) Culture conditions and sampling

*Phaeodactylum tricornutum* Bohlin (UTEX 646) was grown in batch cultures in 200 ml of f/2 prepared with artificial seawater [27]. The growth medium was supplemented with  $\text{NaHCO}_3$  at a final concentration of 11.9 mM. The concentration of nitrate was 10 mM. The algae were grown in 500 ml Erlenmeyer flasks containing 200 ml of growth medium. The flasks were continuously agitated at 100 r.p.m. Cells were irradiated at a photon flux density of  $300 \mu\text{mol photon m}^{-2} \text{s}^{-1}$  as medium light (ML) using cool-white fluorescent tubes (Philips Master TLD 90 DE lux

58 W/965 and Osram L58/77 FLUORA). After 5 days of culture, some of the flasks were transferred to LL and some to HL. The rest, which remained under ML, were used as controls. The intensities of optimal and stressful light were determined using Photosynthesis-Energy curves (see electronic supplementary material, Data SD1). In the manuscript, the day at which cultures were shifted is denoted as day 0. The photon flux densities were measured in an Erlenmeyer filled with growth medium using a  $4\pi$  waterproof light probe (Walz, Germany) connected to a Li-Cor 189 quantum metre [28].

The cycle was 12 L : 12 D and the growth temperature was  $21^\circ\text{C}$ . Cell counting was carried out regularly using a Neubauer haemocytometer and growth rate was obtained after fitting growth kinetics with the sigmoid equation using the freeware Curve expert (<http://www.curveexpert.net/>).

### (b) Photosynthetic and respiratory activities

Photosynthetic and respiratory activities were measured at  $21^\circ\text{C}$  in the light and in the dark using a fibre optic oxygen metre (Pyrosience® FireSting  $\text{O}_2$ , Germany) using a diatom suspension (1.5 ml). Calculated values were normalized for cell density. To avoid  $\text{CO}_2$  shortage during measurements, the cultures were provided with  $\text{NaHCO}_3$  (final, 4 mM per stock, 0.2 M) [29].

### (c) Chlorophyll and carotenoids isolation and quantification

Chlorophyll and carotenoids were extracted and quantified according to the methods described in Jeffrey [30]. Briefly, the samples were collected every day at the same time during the light phase. The cell suspension was centrifuged at  $4^\circ\text{C}$ , 16000g for 5 min (Eppendorf® Centrifuge 5415R). The supernatant was removed; the pigments were extracted with 100% acetone ( $4^\circ\text{C}$ ) (LABOSI® AR) by grinding (held in an ice-bath) and in darkness as recommended in Schoefs [31]. The extract was then quantitatively transferred to centrifuge tube and incubated for at least 4 h at  $4^\circ\text{C}$  in the dark. The full absorption spectrum of the pigment extract solution was recorded between 800 and 400 nm (Perkin Elmer® Lambda-25). The chlorophyll (Chl) *a* and Chl *c* concentrations were calculated according to Jeffrey [30].

$$\text{Chlorophyll } a = 11.77(\text{A}665 \text{ nm} - \text{A}750 \text{ nm}) - 0.82(\text{A}650 \text{ nm} - \text{A}750 \text{ nm}).$$

$$\text{Chlorophyll } c = 26.27(\text{A}650 \text{ nm} - \text{A}750 \text{ nm}) - 3.52(\text{A}665 \text{ nm} - \text{A}750 \text{ nm}).$$

The total carotenoid amount was calculated using the following equation:

$$\text{carotenoids} = \frac{[(\text{A}443 \text{ nm} - \text{A}750 \text{ nm}) - (21.5 \times 10^{-3} \text{ Chl } a) - (369.1 \times 10^{-3} \text{ Chl } c)]}{166.0 \times 10^{-3}}.$$

### (d) Chlorophyll fluorescence yield measurement

The variations of the chlorophyll fluorescence yield were measured and analysed according to Roháček *et al.* [22]. In brief, the chlorophyll fluorescence yield was monitored at the growth temperature after a dark-adaptation period (15 min).  $F_0$  was recorded under a weak modulated light (less than  $15 \mu\text{mol PAR m}^{-2} \text{s}^{-1}$ , 800 Hz). The sample was illuminated during a 7 min non-saturating white actinic radiation with a photon flux density corresponding to the growth photon flux density (KL 1500; H.Walz, Germany). At the end of the actinic illumination, the dark relaxation of the chlorophyll fluorescence yield was recorded in order to allow quenching analysis. For each sample, the minimum ( $F_0$ ,  $F_0'$ ,  $F_0''$ ), maximum ( $F_M$ ,  $F_M'$ ,  $F_M''$ ) and maximum variable ( $F_V$ ,  $F_V'$ ,  $F_V''$ ) were recorded. To avoid  $\text{CO}_2$

shortage during measurements, the cultures were provided with  $\text{NaHCO}_3$  (final, 4 mM per stock, 0.2 M) [22]. The photon flux density used for saturating pulses was  $1200 \mu\text{mol PAR m}^{-2} \text{s}^{-1}$ .

### (e) Determination of lipid and protein content

Total lipid content was extracted using  $10^8$ – $10^9$  cells and was determined by the gravimetric method (Mettler Toledo M5 25–60C) and the content expressed in picograms per cell [32]. Total protein content was quantified using the Bradford method [33].

### (f) Quantification of intracellular carbon and cellular carbon quota

Cell carbon quota ( $Q_C$ ) was determined using a CN elemental analyser (EAGER 300, Thermo Scientific). Samples were filtered through precombusted Whatman GF/C glass filters under gentle vacuum (50 mm Hg) and dried at  $70^\circ\text{C}$  for 48 h. The volume of solution filtered was adjusted to have either 0.1 or  $0.3 \times 10^8$  cells per filter.

### (g) Primer design, real-time quantitative PCR and analyses

A total of 33 enzymes involved in carbon metabolism pathways in *P. tricornutum* were selected and the corresponding genes/isogenes (of 74) coding for each enzyme (electronic supplementary material, table SD2) were searched in genomic data using diatomcyc: <http://www.diatomcyc.org>; JGI portal: <http://genome.jgi.doe.gov/>; BLAST: <http://blast.ncbi.nlm.nih.gov/Blast.cgi>. Primers were designed using Primer Express v. 2.0 (Applied Biosystems, Foster City, CA, USA). In three points of sampling (figure 1) mRNA extractions were performed using the Spectrum Total RNA kit (Sigma Aldrich) protocol with on-column DNase digestion (Sigma-Aldrich). RNA concentrations of samples were determined by UV absorption at 280/260 nm (Nanodrop).

Real-time PCR reactions were performed using a Step One Plus apparatus (Applied Biosystems) with the Gotaq QPCR Master Mix (Promega). The threshold cycle ( $C_t$ ) was determined by the Step One Plus v. 2.1 software. The efficiency of the PCR reaction was calculated for each gene using the  $C_t$  slope method, which involves generating a dilution series of the target template and determining the  $C_t$  value for each dilution. A plot of  $C_t$  versus  $\log(\text{concentration})$  was constructed and efficiency ( $E$ ) expressed as  $E = 10^{(1/\text{slope})}$ . Efficiencies calculated for all genes ( $90 \leq E \leq 110$ ) indicated correct PCR reactions without inhibition [34].

Amplified products of the expected sizes were excised from agarose gel and purified using the QIAEX II gel extraction kit (Qiagen), then cloned into pGEMT plasmid vector (Promega) and sequenced by Beckman Coulter Genomics (Sanger sequencing). BLAST analysis confirmed the sequence identification. Out of the 12 housekeeping gene (HKG) candidates, the most stable (*tbp*, *ubi* and *rps*) were selected due to high  $C_t$  standard deviation (greater than 1) and weak pairwise correlations ( $p > 0.05$ ) compared with the 10 others ( $p < 0.001$ ). The selected HKG were used as the endogenous control genes to normalize the expression of the 74 target genes, using the Bestkeeper Software [35]. The calculation of the relative expression (RE) was based on the comparative  $C_t$  method and calculated as  $\text{RE} = ((E_{TC})^{\Delta C_t} / (E_{HKG})^{\Delta C_t}) / ((E_{HKG})^{\Delta C_t} / (E_{HKG})^{\Delta C_t})$  with  $\Delta C_t = C_{t\text{ML}} - C_{t\text{sample}}$  [36]. In all conditions, ML was used as control and heatmaps with  $\log_2(\text{RE})$  were performed using Netwalker 1.0.

### (h) Statistical analysis

Statistical analyses for physiological data were performed with Student's *t*-test, and  $p \leq 0.05$  was considered statistically significant.

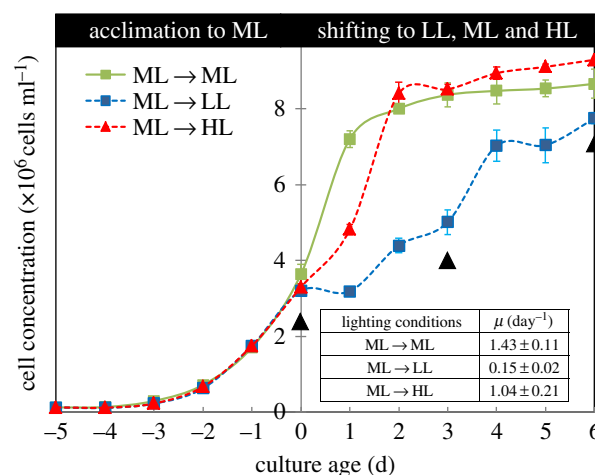


**Figure 1.** Time courses of cell density of cultures developing before and after the light shift. Before being transferred (day 0) to 30 (LL) or 1000 (HL)  $\mu\text{mol m}^{-2} \text{s}^{-1}$ , cultures were developed under  $300 \mu\text{mol m}^{-2} \text{s}^{-1}$  (ML). Light shift was performed at the middle of the exponential phase (day 5), after cells acclimated to ML. The shifted cultures presented typical growth phases, i.e. lag, exponential and plateau, whereas the non-shifted cultures continued to grow until plateau phase. The sampling time of the cultures after light shift is shown using black arrows. (Online version in colour).

## 3. Results and discussion

To get insights on the mechanisms involved in diatom photoacclimation, ML photoacclimated diatoms were subjected to a sudden light shift to LL or HL. In the ocean, *Phaeodactylum* is a taxon usually found in coastal waters and ponds. Near the surface, e.g. 20 cm depth, they can be exposed to photon flux densities as high as  $1500 \mu\text{mol m}^{-2} \text{s}^{-1}$  [37]. This high irradiance generally corresponds to full sunlight [38]. As diatoms can cope with wide variation in irradiance [39], the range used in the present study can be considered as that of natural conditions for *P. tricornutum*. Transcriptional regulation of selected genes coding for enzymes involved in carbon metabolism, change in pigment, lipid and protein amounts as well as in the efficiency of photosynthesis, respiration and light energy dissipation were analysed in the material harvested immediately before the light shift and 3 and 6 days after the light shift. Based on these measurements we observed rearrangements of carbon metabolism towards the production of phosphoenolpyruvic acid (PEP) and/or pyruvate. These intermediates were used differently by the cell as a function of the photon flux density. Of most interest, under HL, the genes coding for the synthesis of aromatic amino acids and phenolic compounds were upregulated.

### (a) *Phaeodactylum tricornutum* adjusts its physiological processes to new lighting conditions

Light is a major factor regulating the development of microalgae [2]. In this study, the impacts of a fast change from optimal growth light intensity (ML) to stressful light intensities (LL and HL) on growth, physiology and expression level of genes coding for enzymes involved in the carbon metabolism of the diatom *P. tricornutum* are followed.

Qualitatively, the same modifications in the pigment amount were observed under the three photon flux densities: the amounts of Chl *a* and total carotenoids increased during

**Table 1.** Cellular carbon quota, carbon immobilized in the culture and relative amount of carbon remaining in the culture.

measured and calculated parameters	lighting conditions	time of sampling		
		shift	shift + 3 days	shift + 6 days
$Q_C$ (pg cell <sup>-1</sup> )	300 → 300	12.2 ± 0.1	9.7 ± 0.3	9.6 ± 0.10
	300 → 30	—	10.7 ± 0.3	10.0 ± 0.4
	300 → 1000	—	8.5 ± 0.1	9.00 ± 0.1
carbon immobilized in the culture (mg)	300 → 300	8.8 ± 0.2	15.5 ± 0.4	16.6 ± 1.7
	300 → 30	—	9.39 ± 0.5	14.1 ± 0.4
	300 → 1000	—	14.2 ± 0.4	16.4 ± 0.2
relative amount of carbon remaining in the culture (%)	300 → 300	62 ± 8	32 ± 2	27 ± 7
	300 → 30	—	59 ± 2	38 ± 2
	300 → 1000	—	38 ± 4	28 ± 1

the period of investigations, reflecting the need to harvest more light when the number of cells was increasing. This is corroborated by the decrease of the Chl *a*/Chl *c* ratio and the increase of total carotenoids/Chl *a* ratio, two proxies reflecting the size of the light-harvesting antenna [40–42] (see electronic supplementary material, Data SD3) and consequent development of more thylakoid membranes [43]. While not studied, the carotenoid composition may have been modified differently under the photon flux densities used here [44]. For instance, only very high photon flux densities trigger the synthesis of the xanthophyll cycle violaxanthin–antheraxanthin–zeaxanthin carotenoids [45]. Quantitatively, the variations were the most intense in the cells shifted to LL (see electronic supplementary material, Data SD3), indicating that these cells were severely deficient in photons. Accordingly, the photosynthetic activity remained weak. To sustain the cell with reductants and energy, the respiratory activity was increased indicating the use of a suitable intracellular carbon pool as suggested in Post *et al.* [46] (see electronic supplementary material, Data SD4 and Data SD5). The use of an intracellular carbon pool would explain the lowering of the  $Q_C$  values after the light shift. At that moment only 40% of the initial carbon content of the culture was consumed (table 1). Altogether, cells were dividing under LL at a lower rate than under ML and HL, resulting in a lower total cell number in the plateau phase than under the two other light intensities (inset in figure 1). Reaching the stationary phase was essentially due to the reduction of carbon availability in the culture (figure 1).

Three days after the shift to HL, the cell quotas of Chl and total carotenoid of diatoms were lower than under ML and the size of the light-harvesting antenna was reduced. The destructure of the pigment-protein complexes is a process that may release free Chl in the chloroplast. The capacity of free tetrapyrroles to generate reactive oxygen species (ROS) is a well-established process [47] that can be limited if the Chl production is slowed down together with the activation of ROS detoxification mechanisms. Accordingly, Nymark *et al.* [9] have reported a decrease in the expression of the genes coding the enzymes of the Chl biosynthetic pathway and an increase of the expression of the genes coding enzymes involved in ROS detoxification. The expression of cGAPDH has been linked to stress conditions (temperature: [48], heavy metals: [49]). The higher expression observed

for this gene under LL and HL compared with ML, especially after 6 days, confirms that the diatoms were grown under stress conditions. At the end of the period studied, the level of pigments is similar to that found in diatoms grown under ML (see electronic supplementary material, Data SD3). Photosynthesis was increased, while keeping respiration unchanged (see electronic supplementary material, Data SD4 and Data SD5). Altogether, these results are in line with earlier reports [9,50,51] and confirm that growth rate is dependent upon the daily light dose received by the microalgae [3]. Despite the fact that the cells had more photons at their disposal under HL conditions, the cultures did not produce more biomass than under ML (figure 1). The estimation of the C consumed by the culture indicated that the stationary phase under HL was also due to the reduction of carbon availability as more than 70% had been used (table 1). The management of light energy by the photosynthetic apparatus can be studied *in vivo* through recording the variations of the chlorophyll fluorescence yield during and after an actinic irradiation (for review, see [52]). Analyses of the chlorophyll fluorescence yield indicated that the fractions of PSII reaction centres (parameter  $qP$ ) remaining open by HL was weak. The absorption of an excess of photons triggers mechanisms of energy dissipation as heat [52]. These mechanisms are collectively referred to as non-photochemical quenching because they lower the chlorophyll fluorescence yield [52]. The related parameters  $qN$  and  $q0$  reflect the excess radiation converted to heat during actinic radiation. The large increase of  $q0$  and  $qN$  parameters when compared with ML conditions indicates that the photons in excess are dissipated as heat. Rohacek *et al.* [22] established that in diatoms three main mechanisms (i.e.  $qNf$ ,  $qNi$  and  $qNs$ ), differing by their rate constant ( $s$ ,  $min$  and  $h$  time-scale, respectively) and intensity, participate in  $qN$ .  $qNi$  is linked to the relaxation of the  $\Delta pH$  gradient across thylakoids and the reversal of the xanthophyll cycle, i.e. the conversion of the xanthophyll diadinoxanthin to diatoxanthin upon lumen acidification (for a review, see [53]).  $qNs$  quantifies the stage of photoinhibition caused by the high light exposure. The last component,  $qNf$ , seems to reflect fast conformational changes within thylakoid membranes in the vicinity of the photosystem II complexes. For the control cells, only  $qNf$  increased significantly, suggesting that under this light intensity, the need for a mechanism of light energy

dissipation is weak. Compared with ML conditions, both  $q_{Ni}$  and  $q_{Ns}$  have significantly increased whereas  $q_{Nf}$  remained unchanged (see electronic supplementary material, table SD5.3). This result fits well with the fact that under ML photon flux density, the expression of the genes coding the proteins of the PSII reaction centre (*psbA*: D1, and *psbD*: D2) and those catabolizing the photodamaged PSII reaction center (*FTSH1* and *FTSH2*) remain stable [9]. The gene *psbD* codes the photosystem II reaction centre D2 protein, one of the proteins with the highest turnover rate under stress conditions [54]. Because  $q_{Ns}$  is linked to photoinhibition, the significant increase in this parameter suggests that the excess of light energy activates both the xanthophyll cycle and photoinhibition. A higher level of photoinhibition would explain the reduced growth rate of the cultures transferred to HL when compared with ML (figure 1).

During the transition from ML to LL, the non-photochemical quenching relaxes because the requirement for excess absorbed light energy vanished under this photon flux density.

### (b) Light shift changes the pattern of gene expression

Metabolic reactions and gene regulation are two primary processes of cells leading carbon allocation to different pathways. In response to environmental changes, cells adjust the regulatory programmes and shift the metabolic states as reflected in their physiology [55]. To study the crosstalk between light acclimation and gene regulation, we exposed the cells under sudden light stress after acclimation to ML. A schematic of the central carbon metabolism is presented in the electronic supplementary material, Data SD6. Despite the fact that mRNA abundance is not always correlated with protein levels and enzyme activities [55], it is frequently used as a good indicator of metabolic modifications [56]. Based on the measurements, the expression pattern of genes/isogenes encoding different enzymes in carbon metabolism pathways was variable according to light intensity and acclimation period after light shift (expression pattern of the genes is shown in figure 2 and  $\log_2$  values of the expression ratios are displayed in electronic supplementary material, Data SD7).

### (c) Towards acclimation to high light

After the shift to HL, diatoms have an increased photosynthetic capacity (see electronic supplementary material, Data SD4) that would have generated additional ATP and NADPH. This would allow an increase of Calvin cycle activity (also supported by the increase of mRNA expression of *FbaC1*: 3.9-fold, *FBPC3*: 4.3-fold, *TPI\_2*: 3.5-fold, *RbcL*: 2.2-fold), providing enough  $CO_2$  is imported into the chloroplast. In our growing conditions, the diatoms were progressively starved of  $CO_2$  and 6 days after the shift, approximately 80% of the initial  $CO_2$  was consumed (table 1). To overcome the decrease of carbon supply, marine diatoms trigger carbon concentration mechanisms (CCM). CCM can operate through two pathways, the so-called biochemical and biophysical CCM. The biochemical mechanism consists of the fixation of solubilized  $CO_2$  (i.e.  $HCO_3^-$ ) using C4-type metabolism. The biophysical CCM relies on carbonic anhydrases that facilitate  $CO_2$  transport and solubilization from the growth medium to the pyrenoid, in which RuBisCO is concentrated [57]. In our conditions, the upregulation of several other genes coding enzymes of the biochemical CCM suggests an

enforcement of the  $CO_2$  import capacity, in line with the carbon shortage conditions. These enzymes are the mitochondrial pyruvate carboxylase (PYC1: 4.5-fold) and the endoplasmic reticulum PEP carboxylases (PEPC1: 2.6-fold, PEPC2: 2.5-fold, PEPCK: 1.4-fold, ME1: 1.3-fold) (figure 2). Genes coding for carbonic anhydrases located in the periplasmic space (CA2: 1.3-fold, CA6: 1.3-fold) and in the pyrenoid (CA3: 1.4-fold) [58] were moderately upregulated 3 days after the light shift and then significantly downregulated 6 days after the shift. These results suggest that the  $CO_2$  import is directed towards the biochemical CCM more than the biophysical CCM. Six days after the shift, the genes coding for enzymes of the Calvin cycle were downregulated in response to  $CO_2$  shortage in the growth medium.

The upregulation of the gene coding for the chloroplast-located *PGAM4* (1.2-fold) suggests that the 3-phospho-D-glycerate (3PG) was directed towards PEP formation (figure 2). PEP is at one side of the chloroplast pyruvate hub [59], serving as a precursor of pyruvate or for the shikimate pathway. This possibility is likely because of the downregulation of the gene *PK1* coding for the enzyme transforming PEP to pyruvate and the upregulation of several genes in the shikimate pathway (*ATIG*: 6.4-fold, *SK*: 2.8-fold, *AroB*: 1.3-fold) 3 days after the shift (figure 2). Six days after the shift, the upregulation of the shikimate pathway was even higher (*AroA*: 3.7-fold, *AroB*: 4.1-fold, *EPSP*: 3-fold, *ATIG*: 2.5-fold) compared with ML and strengthened by the upregulation of the gene *PPDK* that codes the enzyme converting pyruvate to PEP (figure 2). Phenolic compounds that are eventually produced by the shikimate pathway form an important group of natural products involved in responses to different kinds of biotic and abiotic stresses [60]. A few reports have dealt with their biosynthesis and role in diatoms. For instance, Rico *et al.* [61] reported their involvement in the protection of *Phaeodactylum* against metal toxicity such as copper or iron. Phenolic compounds have the capacity to absorb near UV and blue wavelengths [62] and display an antioxidant role in diatoms as well as in higher plants [63]. Such an activity might be required to protect the cells from ROS formation during size reduction of the light-harvesting antenna. Concomitantly, part of the PEP pool could be used, through pyruvate formation, for lipid and/or amino acid syntheses or, be transported to the other compartments for oxidation to  $CO_2$  via the Krebs cycle [64]. This possibility is illustrated by the upregulation of the gene *PEPC1* (1.6-fold) that encodes the enzyme converting PEP to oxaloacetate (OAA) in the endoplasmic reticulum and/or periplasmic space. The OAA produced could be transported into the mitochondria [65] to enter into the Krebs cycle. However, it could not be a crucial flux of PEP because no significant increase in respiration was detected (compared with ML).

Six days after the light shift to HL, the diatom cells contained more proteins and lipids than under ML (electronic supplementary material, figure SD8). Because of the downregulation of *PK1* (−1.4-fold) and the upregulation of *PPDK* (1.5-fold) genes, and under the hypothesis that these levels of expression reflect the amount of the corresponding enzymes, the increase of lipids and proteins must be performed through an import of pyruvate from other compartments, i.e. mitochondria and cytoplasm [66], using adequate transporters [65,67]. This hypothesis is supported by the upregulation of cytosolic glycolytic enzymes (*PK2*: 1.2-fold, *GPI*: 8.3-fold, *GPI\_1*: 1.6-fold and *FBP*: 1.5-fold) and the mitochondrial glycolytic

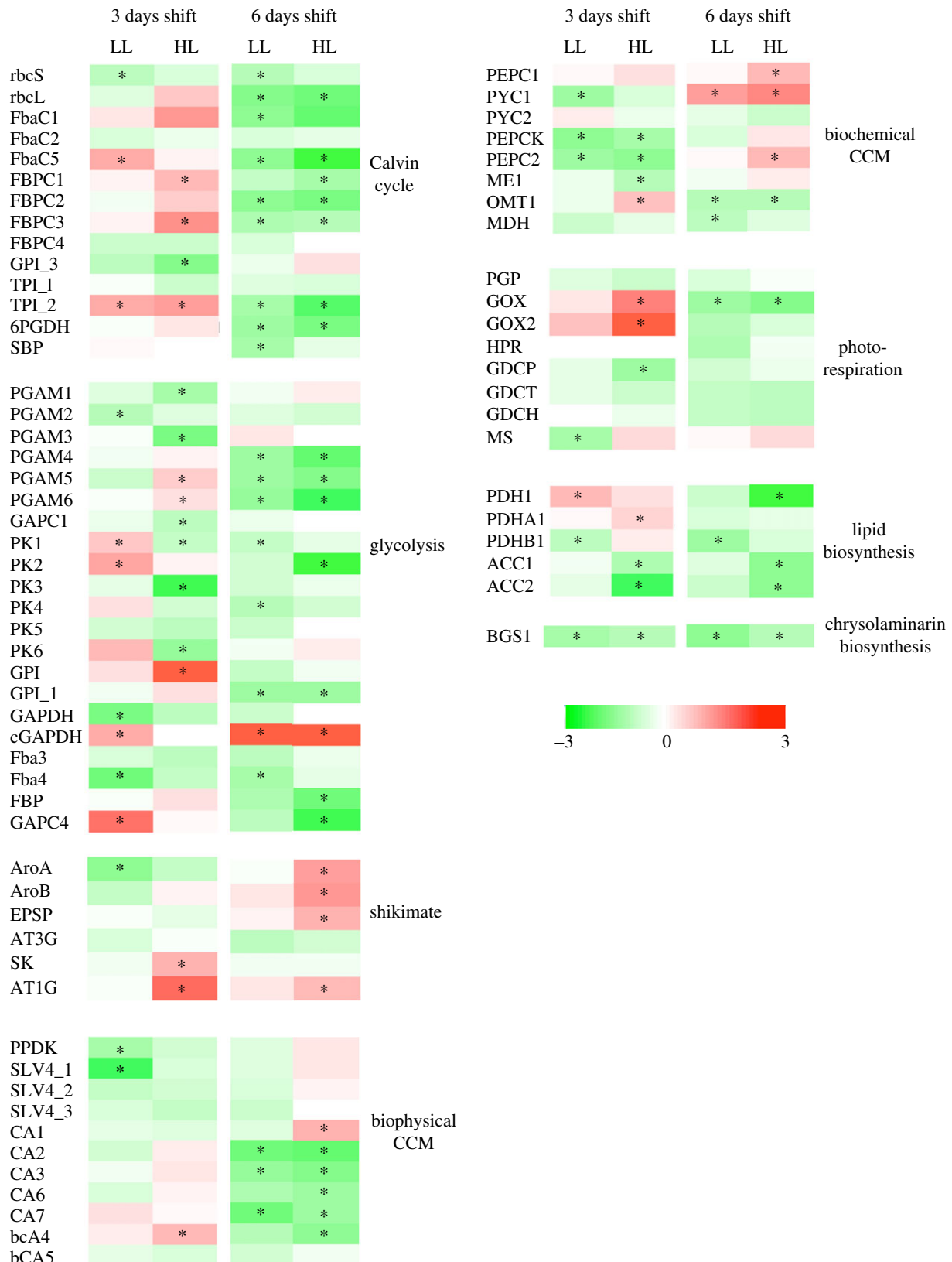


**Figure 2.** Dysregulated heat map showing the expression pattern of 74 genes related to carbon metabolic pathways, with the greatest differences in expression (red, high; green, low). Columns represent 3 and 6 days after shift from medium light (ML) to low light (LL) and high light (HL). In both conditions, ML is used as calibrator. Asterisks indicate genes that are significantly regulated compared with ML ( $p < 0.05$ ).

pathway (*GAPC4*: 1.2-fold, *PGAM5*: 2-fold and *PGAM6*: 1.5-fold) (figure 2). These upregulations were not observed 6 days after the shift except for the *cGAPDH* gene that was expressed 100 times more (figure 2).

Three days after the shift, several genes coding for enzymes involved in photorespiration (peroxisome: *GOX*

and *MS*; mitochondria: *GOX2*) were upregulated (5.2-, 1.7- and 18.1-fold, respectively, when compared with ML) (figure 2). These upregulations would favour glyoxylate and succinate synthesis that, in turn, can directly or indirectly enter the Krebs cycle to form intermediate metabolites for anabolic pathways like amino acid synthesis [68]. An increase

of the photorespiratory activity would fit with the lowering of  $Q_C$  after the light shift from ML to HL (table 1).

#### (d) Towards acclimation to low light

Diatom cells shifted to LL were accumulating similar amounts of lipids and proteins (electronic supplementary material, figure SD8) compared with ML. This suggests that the fixed carbon was consumed to increase the pigment content as well as to produce substrates for respiration, which was more intense under LL (electronic supplementary material, figure SD3). In the first place, pyruvate formation was favoured 3 days after the light shift by upregulating genes coding for enzymes involved in the glycolytic pathways located in mitochondria (*GAPC4*: 6.1-fold, pyruvate kinase *PK6*: 2.6-fold), chloroplast (*PK1*: 2.1-fold) and cytosol (*PK2*: 3.5-fold, *PK4*: 1.5-fold, *GPI*: 1.6-fold, *cGAPDH*: 3.1-fold). Six days after the light shift, the *cGAPDH* gene was the most upregulated gene (37.5-fold), as under HL (figure 2). The fate of pyruvate was different under LL compared to HL. This is supported by the upregulation of *TPI\_2* (3.0-fold), *FbaC5* (3.1-fold) and *PYC2* (1.4-fold) genes coding for chloroplastic enzymes involved in glyceraldehyde 3-phosphate, dihydroxyacetone phosphate and OAA formation 3 days after the light shift. Six days after the light shift, the *PYC1* gene, which codes for an enzyme converting pyruvate to OAA, was upregulated (3.6-fold), as under HL (figure 2). Upon transport, these intermediates can be used to feed the Krebs cycle. Interestingly, under LL, all the genes coding enzymes involved in the biophysical CCM were downregulated, probably participating in the decrease of the photosynthetic activity (electronic supplementary material, figure SD4).

## 4. Conclusion

The transcriptome of *P. tricornutum* has been studied in a few contexts, such as silicon metabolism [69], short-term light acclimation [9], salt and temperature variation [70], carbon fixation, storage and utilization [71] and nitrogen stress [72]. To date, molecular mechanisms behind light acclimation during diatom growth remain largely unknown and growth-related modifications in gene expression induced by different light intensities in *P. tricornutum* have not yet been described. Exposure of cells to different growth light regimes after acclimation to ML induced composite acclimation patterns manifesting in strong alterations in cell biology, physiology and biochemical acclimation. In the growing conditions used here, a CO<sub>2</sub> shortage is mostly responsible for the cultures attaining the stationary phase. This CO<sub>2</sub> shortage

triggered the biochemical CCM regardless of the photon flux density to which the cells were transferred. Owing to the observed downregulation of the carbonic anhydrases, LL shifted cells were facing CO<sub>2</sub> starvation, which is reflected in the reduction of their photosynthesis activity. Regardless of the mechanism used, i.e. the lighting conditions to which the cells were transferred, the carbon metabolism was directed towards the production of PEP and/or pyruvate. This may have involved cooperation between the different cell compartments. Remarkably, the fate of pyruvate was different with respect to the light intensity. Under LL, it could be used to synthesize compounds that would, in turn, be used to keep the respiratory activity high. Doing so, enough ATP would be generated to sustain growth and pigment synthesis. Under HL, part of the fixed carbon was used for the accumulation of lipids and proteins. Interestingly, the genes coding for the synthesis of aromatic amino acids and phenolic compounds, i.e. the shikimate pathway, are activated under HL. In photosynthetic organisms, phenolic compounds are involved in responses to biotic or abiotic stress conditions but only a few reports are dedicated to diatoms. Higher expression of the genes under HL might indicate their importance in protecting against excess light damage. Further studies are needed to better understand the function of the shikimate pathway in *Phaeodactylum*. Altogether, this study provides results on the molecular and physiological mechanisms used by diatoms to acclimate to lighting conditions. Beyond their interest for the understanding of the physiology and ecology of diatoms, our data might be of interest for the development of biotechnological processes aiming to produce proteins and/or pigments.

**Data accessibility.** Provided within the electronic supplementary material. Further data are accessible upon request to the corresponding authors.

**Authors' contributions.** P.H., J.M., B.S., V.M.-J. designed the research; P.H., W.B., B.M., B.H., E.L., G.W.-C., A.C.-M., J.M. performed research; P.H., B.H., G.W.-C., A.C.-M., M.Z., G.B., J.M., B.S. analysed the data and P.H., J.M., B.S. wrote the paper.

**Competing interests.** We have no competing interests.

**Funding.** P.H. thanks the doctoral school Végétal Environnement Nutrition Alimentation Mer, the Collège doctoral of the University of Le Mans and the Region Pays de la Loire for their financial support. P.H., J.M. and B.S. thanks the Ministry of Foreign Affairs of the French Republic for financial support through the programme Partenariat Hubert Curien Gundishapur. V.M.J. was supported by Centre National de la Recherche Scientifique (CNRS) and University of Nantes.

**Acknowledgements.** P.H. thanks the Isfahan University of Technology for a sabbatical program. A.C.M. and G.W.C. thank Vony Rabesaotra, University of Nantes, for her technical assistance. The authors thank Prof. Richard Gordon for his careful reading of the text.

## References

- Geider RJ, Intyre HL, Kana TM. 1998 A dynamic regulatory model of phytoplanktonic acclimation to light, nutrients and temperature. *Limnol. Oceanogr.* **43**, 679–694. (doi:10.4319/lo.1998.43.4.679)
- Darko E, Heydarizadeh P, Schoefs B, Sabzaljan MR. 2014 Photosynthesis under artificial light: the shift in primary and secondary metabolites. *Phil. Trans. R. Soc. B* **369**, 20130243. (doi:10.1098/rstb.2013.0243)
- Orefice I *et al.* 2016 Light-induced changes in the photosynthetic physiology and biochemistry in the diatom *Skeletonema marinoi*. *Algal Res.* **17**, 1–13. (doi:10.1016/j.algal.2016.04.013)
- Kooistra WHCF, Gersonde R, Medlin LK, Mann DG. 2007 The origin and evolution of the diatoms: their adaptation to a planktonic existence. In *Evolution of planktonic photoautotrophs* (eds PG Falkowski, AH Knoll), pp. 207–249. Burlington, MA: Academic Press.
- Reeves S, McMinn A, Martin A. 2011 The effect of prolonged darkness on the growth, recovery and survival of Antarctic sea ice diatoms. *Polar Biol.* **34**, 1019–1032. (doi:10.1007/s00300-011-0961-x)

6. Arrigo KR, Perovich DK, Pickart RS. 2012 Massive phytoplankton blooms under arctic sea ice. *Science* **336**, 1408. (doi:10.1126/science.1215065)
7. Jallet D, Caballero MA, Gallina AA, Youngblood M, Peers G. 2016 Photosynthetic physiology and biomass partitioning in the model diatom *Phaeodactylum tricorutum* grown in a sinusoidal light regime. *Algal Res.* **18**, 51–60. (doi:10.1016/j.algal.2016.05.014)
8. Bowler C *et al.* 2008 The *Phaeodactylum* genome reveals the evolutionary history of diatom genomes. *Nature* **456**, 239–244. (doi:10.1038/nature07410)
9. Nymark M, Valle KC, Brembu T, Hancke K, Winge P, Andresen K, Johnsen G, Bones AM. 2009 An integrated analysis of molecular acclimation to high light in the marine diatom *Phaeodactylum tricorutum*. *PLoS ONE* **4**, e7743. (doi:10.1371/journal.pone.0007743)
10. Nymark M, Valle KC, Hancke K, Winge P, Andresen K, Johnsen G, Bones AM, Brembu T. 2013 Molecular and photosynthetic responses to prolonged darkness and subsequent acclimation to re-illumination in the diatom *Phaeodactylum tricorutum*. *PLoS ONE* **8**, e58722. (doi:10.1371/journal.pone.0058722)
11. Valle KC, Nymark M, Aamot I, Hancke K, Winge P, Andresen K, Johnsen G, Brembu T, Bones AM. 2014 System responses to equal doses of photosynthetically usable radiation of blue, green, and red light in the marine diatom *Phaeodactylum tricorutum*. *PLoS ONE* **9**, e114211. (doi:10.1371/journal.pone.0114211)
12. Rosenwasser S *et al.* 2014 Mapping the diatom redox-sensitive proteome provides insight into response to nitrogen stress in the marine environment. *Proc. Natl Acad. Sci. USA* **111**, 2740–2745. (doi:10.1073/pnas.1319773111)
13. Ge F, Huang W, Chen Z, Zhang C, Xiong Q, Bowler C, Yang J, Xu J, Hu H. 2014 Methylcrotonyl-CoA carboxylase regulates triacylglycerol accumulation in the model diatom *Phaeodactylum tricorutum*. *Plant Cell* **26**, 1681–1697. (doi:10.1105/tpc.114.124982)
14. Alipanah L, Rohloff J, Winge P, Bones AM, Brembu T. 2015 Whole-cell response to nitrogen deprivation in the diatom *Phaeodactylum tricorutum*. *J. Exp. Bot.* **66**, 6281–6296. (doi:10.1093/jxb/erv340)
15. Muhseen ZT, Xiong Q, Chen Z, Ge F. 2015 Proteomics studies on stress responses in diatoms. *Proteomics* **15**, 3943–3953. (doi:10.1002/pmic.201500165)
16. Griffiths DJ. 1973 Factors affecting photosynthetic capacity of laboratory cultures of diatom *Phaeodactylum tricorutum*. *Mar. Biol.* **21**, 91–97. (doi:10.1007/BF00354603)
17. Raven JA, Geider RJ. 2003 Adaptation, acclimation and regulation in algal photosynthesis. In *Photosynthesis of algae* (eds AWD Larkum, S Douglas, JA Raven), pp. 385–412. Dordrecht, The Netherlands: Kluwer Academic Publishers.
18. Bailleul B, Rogato A, Martino A, Coesel S, Cardol P, Bowler C, Falciatore A, Finazzi G. 2010 An atypical member of the light-harvesting complex stress related protein family modulated diatom response to light. *Proc. Natl Acad. Sci. USA* **107**, 18 214–18 219. (doi:10.1073/pnas.1007703107)
19. Lepetit B, Sturm S, Rogato A, Gruber A, Sachse M, Falciatore A, Kroth PG, Lavaud J. 2013 High light acclimation in the secondary plastids containing diatom *Phaeodactylum tricorutum* is triggered by the redox state of the plastoquinone pool. *Plant Physiol.* **161**, 853–865. (doi:10.1104/pp.112.207811)
20. Wu H, Roy S, Alami M, Green BR, Campbell DA. 2012 Photosystem II photoinactivation, repair, and protection in marine centric diatoms. *Plant Physiol.* **160**, 464–476. (doi:10.1104/pp.112.203067)
21. Dong YL, Jiang T, Xia W, Dong HP, Lu SH, Cui L. 2015 Light harvesting proteins regulate non-photochemical fluorescence quenching in the marine diatom *Thalassiosira pseudonana*. *Algal Res.* **12**, 300–307. (doi:10.1016/j.algal.2015.09.016)
22. Roháček K, Bertrand M, Moreau B, Jacqueline J, Caplat C, Morant-Manceau A, Schoefs B. 2014 Relaxation of the non-photochemical chlorophyll fluorescence quenching in diatoms: kinetics, components and mechanisms. *Phil. Trans. R. Soc. B* **369**, 20130241. (doi:10.1098/rstb.2013.0241)
23. Sayanova O, Mimouni V, Ulmann L, Morant-Manceau A, Pasquet V, Schoefs B, Napier JA. 2017 Modulation of lipid biosynthesis by stress in diatoms. *Phil. Trans. R. Soc. B* **372**, 20160407. (doi:10.1098/rstb.2016.0407)
24. Levering J, Dupont CL, Allen AE, Palsson BO, Zengler K. 2017 Integrated regulatory and metabolic networks of the marine diatom *Phaeodactylum tricorutum* predict the response to rising CO<sub>2</sub> levels. *mSystems* **2**, e00142-16. (doi:10.1128/mSystems.00142-16)
25. Fisher NL, Halsey KH. 2016 Mechanisms that increase the growth efficiency of diatoms in low light. *Photosynthesis Res.* **129**, 183–197. (doi:10.1007/s11120-016-0282-6)
26. Heydarzadeh P, Poirier I, Loizeau D, Ulmann L, Mimouni V, Schoefs B, Bertrand M. 2013 Plastids of marine phytoplankton produce bioactive pigments and lipids. *Mar. Drugs* **11**, 3425–3471. (doi:10.3390/md11093425)
27. Guillard RR, Ryther JH. 1962 Studies of marine planktonic diatoms: I. *Cyclotella nana* and *Detonula confervacea* (Cleve). *Can. J. Microbiol.* **8**, 229–239. (doi:10.1139/m62-029)
28. Tremblin G, Cannuel R, Mouget J, Rech M, Robert JM. 2000 Change in light quality due to a blue-green pigment marenine, released in oyster-ponds: effect on growth and photosynthesis in two diatoms, *Haslea ostrearia* and *Skeletonema costatum*. *J. Appl. Phycol.* **12**, 557–566. (doi:10.1023/A:1026502713075)
29. Lavaud J, Kroth P. 2006 In diatoms, the transthylakoid proton gradient regulates the photoprotective non-photochemical fluorescence quenching beyond its control on the xanthophyll cycle. *Plant Cell Physiol.* **47**, 1010–1016. (doi:10.1093/pcp/pcj058)
30. Jeffrey SW. 1997 Application of pigment methods to oceanography. In *Phytoplankton pigments in oceanography: guidelines to modern methods* (eds SW Jeffrey, RFC Mantoura, SW Wright), pp. 127–167. Paris, France: UNESCO.
31. Schoefs B. 2003 Chlorophyll and carotenoid analysis in food products. A practical case-by-case view. *Trends Anal. Chem.* **22**, 335–339. (doi:10.1016/S0165-9936(03)00602-2)
32. Kendel M, Couzinet-Mossion A, Viau M, Fleurence J, Barnathan G, Wielgosz-Collin G. 2011 Seasonal composition of lipids, fatty acids, and sterols in the edible red alga *Grateloupia turuturu*. *J. Appl. Phycol.* **25**, 425–432. (doi:10.1007/s10811-012-9876-3)
33. Bradford MM. 1976 A rapid sensitive method for the quantitation of microgram quantities of protein utilizing the principle of protein-dye binding. *Anal. Biochem.* **72**, 248–254. (doi:10.1016/0003-2697(76)90527-3)
34. Gašparič MB, Cankar K, Želj J, Gruden K. 2008 Comparison of different real-time PCR chemistries and their suitability for detection and quantification of genetically modified organisms. *BMC Biotechnol.* **8**, 26. (doi:10.1186/1472-6750-8-26)
35. Pfaffl MW, Tichopad A, Prgomet C, Neuvians TP. 2004 Determination of stable housekeeping genes, differentially regulated target genes and sample integrity: BestKeeper—Excel-based tool using pairwise correlations. *Biotechnol. Lett.* **26**, 509–515. (doi:10.1023/B:BILE.0000019559.84305.47)
36. Livak KJ, Schmittgen TD. 2001 Analysis of relative gene expression data using real time quantitative PCR and the 2-Ct method. *Methods* **25**, 402–408. (doi:10.1006/meth.2001.1262)
37. Mouget JL, Tremblin G, Morant-Manceau A, Moranças M, Robert JM. 1999 Long-term photoacclimation of *Haslea ostrearia* (Bacillariophyta): effect of irradiance on growth rates, pigment content and photosynthesis. *Eur. J. Phycol.* **34**, 109–115. (doi:10.1080/09670269910001736162)
38. Richardson K, Beardall J, Raven JA. 1983 Adaptation of unicellular algae to irradiance: an analysis of strategies. *New Phytol.* **93**, 157–191. (doi:10.1111/j.1469-8137.1983.tb03422.x)
39. Fogg GE. 1991 The phytoplanktonic ways of life. *New Phytol.* **118**, 191–232. (doi:10.1111/j.1469-8137.1991.tb00974.x)
40. Lamote M, Darko E, Schoefs B, Lemoine Y. 2003 Assembly of the photosynthetic apparatus in embryos from *Fucus serratus* L. *Photosynthesis Res.* **77**, 45–52. (doi:10.1023/A:1024999024157)
41. Nguyen-Deroche TLNN, Caruso A, Le TT, Viet Bui T, Schoefs B, Tremblin G, Morant-Manceau A. 2012 Zinc affects differently growth, photosynthesis, antioxidant enzyme activities and phytochelatin synthase expression of four marine diatoms. *Sci. World J.* **15**, 982957. (doi:10.1100/2012/982957)
42. Schoefs B, Bertrand M, Lemoine Y. 1998 Changes in the photosynthetic pigments in bean leaves during the first photoperiod of greening and the subsequent dark-phase. Comparison between old (10-d-old) leaves and young (2-d-old) leaves.

- Photosynthesis Res.* **57**, 203–213. (doi:10.1023/A:1006000208160)
43. Lepetit B, Goss R, Jakob T, Wilhelm C. 2012 Molecular dynamics of the diatom thylakoid membrane under different light conditions. *Photosynthesis Res.* **111**, 245–257. (doi:10.1007/s11120-011-9633-5)
  44. Kuczynska P, Jemiola-Rzeminska M. 2017 Isolation and purification of all-*trans* diadinoxanthin and all-*trans* diatoxanthin from diatom *Phaeodactylum tricorutum*. *J. Appl. Phycol.* **29**, 79–87. (doi:10.1007/s10811-016-0961-x)
  45. Lohr M, Wilhelm C. 1999 Algae displaying the diadinoxanthin cycle also possess the violaxanthin cycle. *Proc. Natl Acad. Sci. USA* **96**, 8754–8789. (doi:10.1073/pnas.96.15.8784)
  46. Post AF, Dubinsky Z, Wyman K, Falkowski PG. 1985 Physiological responses of a marine planktonic diatom to transitions in growth irradiance. *Mar. Ecol. Progr. Ser.* **25**, 141–149. (doi:10.3354/meps025141)
  47. Schoefs B, Franck F. 2003 Protchlorophyllide reduction: mechanisms and evolution. *Photochem. Photobiol.* **78**, 543–557. (doi:10.1562/0031-8655(2003)078<0543:PRMAE>2.0.CO;2)
  48. Nilo R *et al.* 2010 Proteomic analysis of peach fruit mesocarp softening and chilling injury using difference gel electrophoresis (DIGE). *BMC Genomics* **11**, 43. (doi:10.1186/1471-2164-11-43)
  49. Mench M, Schwitzguébel J, Schroeder P, Bert V, Gawronski S, Gupta S. 2009 Assessment of successful experiments and limitations of phytotechnologies: contaminant uptake, detoxification and sequestration, and consequences for food safety. *Environ. Sci. Pollut. Res.* **16**, 876–900. (doi:10.1007/s11356-009-0252-z)
  50. Beardall J, Morris I. 1976 The concept of light intensity adaptation in marine phytoplankton: some experiments with *Phaeodactylum tricorutum*. *Mar. Biol.* **37**, 377–387. (doi:10.1007/BF00387494)
  51. Geider RJ, Osborne BA, Raven JA. 1986 Growth, photosynthesis and maintenance metabolic cost in the diatom *Phaeodactylum tricorutum* at very low light levels. *J. Phycol.* **22**, 39–48. (doi:10.1111/j.1529-8817.1986.tb02513.x)
  52. Rohacek K, Soukupova J, Bartak M. 2008 Chlorophyll fluorescence: a wonderful tool to study plant physiology and plant stress. In *Plant cell organelles—selected topics* (ed. B Schoefs), pp. 251–284. Trivandrum, India: Research Signpost.
  53. Bertrand M. 2010 Carotenoid biosynthesis in diatoms. *Photosynthesis Res.* **106**, 89–102. (doi:10.1007/s11120-010-9589-x)
  54. Nagao R, Tomo T, Narikawa R, Enami I, Ikeuchi M. 2016 Conversion of photosystem II dimer to monomers during photoinhibition is tightly coupled with decrease in oxygen-evolving activity in the diatom *Chaetoceros gracilis*. *Photosynthesis Res.* **130**, 83–91. (doi:10.1007/s11120-016-0226-1)
  55. Heydarzadeh P, Marchand J, Chenais B, Sabzalian MR, Zahedi M, Moreau B, Schoefs B. 2014 Functional investigations in diatoms need more than transcriptomic approach. *Diatom Res.* **29**, 75–89. (doi:10.1080/0269249X.2014.883727)
  56. Gygi S, Rochon Y, Franza BR, Aebersold R. 1999 Correlation between protein and mRNA abundance in yeast. *Mol. Cell Biol.* **19**, 1720–1730. (doi:10.1128/MCB.19.3.1720)
  57. Hopkinson BM, Dupont CL, Allen AE, Morel FMM. 2011 Efficiency of the CO<sub>2</sub>-concentrating mechanism of diatoms. *Proc. Natl Acad. Sci. USA* **108**, 3830–3837. (doi:10.1073/pnas.1018062108)
  58. Tachibana M, Allen A, Kikutani S, Endo Y, Bowler C, Matsuda Y. 2011 Localization of putative carbonic anhydrases in two marine diatoms, *Phaeodactylum tricorutum* and *Thalassiosira pseudonana*. *Photosynthesis Res.* **109**, 205–211. (doi:10.1007/s11120-011-9634-4)
  59. Shtaida N, Khozin-Goldberg I, Boussiba S. 2015 The role of pyruvate hub enzymes in supplying carbon precursors for fatty acid synthesis in photosynthetic microalgae. *Photosynthesis Res.* **125**, 407–422. (doi:10.1007/s11120-015-0136-7)
  60. Treutter D. 2006 Significance of flavonoids in plant resistance: a review. *Environ. Chem. Lett.* **4**, 147. (doi:10.1007/s10311-006-0068-8)
  61. Rico M, Lopez A, Magdalena Santana-Casiano J, Gonzalez AG, Gonzalez-Davila M. 2013 Variability of the phenolic profile in the diatom *Phaeodactylum tricorutum* growing under copper and iron stress. *Limnol. Oceanogr.* **58**, 144–152. (doi:10.4319/l.2013.58.1.0144)
  62. Kolb CA, Kopecky J, Riederer M, Pfundel EE. 2003 UV screening by phenolics in berries of grapevine (*Vitis vinifera*). *Funct. Plant Biol.* **30**, 1177–1186. (doi:10.1071/FP03076)
  63. Hemalatha A, Parthiban C, Saranya C, Girija K, Anantharaman P. 2015 Evaluation of antioxidant activities and total phenolic contents of different solvent extracts of selected marine diatoms. *Ind. J. Geo-Mar. Sci.* **44**, 1630–1636.
  64. Liaud MF, Litchlé, Apt K, Martin W, Cerff R. 2000 Compartment-specific isoforms of TPI and GAPDH are imported into diatom mitochondria as a fusion protein: evidence in favor of a mitochondrial origin of the eukaryotic glycolytic pathway. *Mol. Biol. Evol.* **17**, 213–223. (doi:10.1093/oxfordjournals.molbev.a026301)
  65. Marchand J, Heydarzadeh P, Schoefs B, Spetea C. 2016 Chloroplast ion and metabolite transport in algae. In *Photosynthesis in algae* (eds AWD Larkum, A Grossman, J Raven), 2nd edn. Berlin, Germany: Springer.
  66. Kroth PG *et al.* 2008 A model of carbohydrate metabolism in the diatom *Phaeodactylum tricorutum* deduced from comparative whole genome analysis. *PLoS ONE* **3**, e1426. (doi:10.1371/journal.pone.0001426)
  67. Hohner R, Aboukila A, Kunz HH, Venema K. 2016 Proton gradients and proton-dependent transport processes in the chloroplast. *Front. Plant Sci.* **7**, 218. (doi:10.3389/fpls.2016.00218)
  68. Kim J, Fabris M, Baart G, Kim MK, Goossens A, Vyverman W, Falkowski PG, Lun DS. 2016 Flux balance analysis of primary metabolism in the diatom *Phaeodactylum tricorutum*. *Plant J.* **85**, 161–176. (doi:10.1111/tpj.13081)
  69. Sapriel G, Quinet M, Heijde M, Jourden L, Tanty V, Luo G, Le Crom S, Lopez PJ. 2009 Genome-wide transcriptome analyses of silicon metabolism in *Phaeodactylum tricorutum* reveal the multilevel regulation of silicic acid transporters. *Plant Cell* **4**, e7458. (doi:10.1371/journal.pone.0007458)
  70. De Martino A, Bartual A, Willis A, Meichenin A, Villazan B, Maheswari U, Bowler C. 2011 Physiological and molecular evidence that environmental changes elicit morphological interconversion in the model diatom *Phaeodactylum tricorutum*. *Protist* **162**, 462–481. (doi:10.1016/j.protis.2011.02.002)
  71. Chauton MS, Winge P, Brembu T, Vadstein O, Bones AM. 2013 Gene regulation of carbon fixation, storage, and utilization in the diatom *Phaeodactylum tricorutum* acclimated to light/dark cycles. *Plant Physiol.* **161**, 1034–1048. (doi:10.1104/pp.112.206177)
  72. Levitan O, Dinamarca J, Zelzouk E, Lun DS, Guerra LT, Kim MK, Kim J, Van Mooy BAS, Bhattacharya D, Falkowski PG. 2015 Remodeling of intermediate metabolism in the diatom *Phaeodactylum tricorutum* under nitrogen stress. *Proc. Natl Acad. Sci. USA* **112**, 412–417. (doi:10.1073/pnas.1419818112)